OT08

Apparent contact angle of oleic acid and triolein on a reverse osmosis membrane in SC-CO_2 environment

Karina Araus, Eileen Santos, Ricardo Couto, Feral Temelli*
Department of Agricultural, Food and Nutritional Science
University of Alberta, Edmonton, Alberta, Canada T6G 2P5
email: feral.temelli@ualberta.ca

ABSTRACT

Although polymeric reverse osmosis membranes are typically used for water purification with high salt rejection rates, they have been also used to separate mixtures of much larger lipid molecules using supercritical carbon dioxide (SC-CO_2). The coupled membrane-SC-CO_2 process is influenced by the operating conditions and the interactions between the lipids, SC-CO_2 and the membrane. To understand these interactions, the wetting phenomena was studied by determining the apparent contact angles (CA_{app}) of oleic acid (OA) and triolein (TO) in air and SC-CO_2 on a commercial SG membrane over time (0-1 s). The atmospheric conditions for testing in air were 22°C/0.1 bar, whereas SC-CO_2 was tested at 40°C/120 bar. Images of the sessile drops were analyzed by the B-spline snake method. The CA_{app} for OA and TO at atmospheric conditions were higher than those under SC-CO_2. At atmospheric conditions, the CA_{app} for OA and TO were 49.74°±0.64° and 56.80°±1.05° at 0 s and 12.26°±1.07° and 13.10°±0.46° at 1 s, respectively. Under SC-CO_2 environment, the CA_{app} for OA and TO were 37.33°±0.27° and 53.92°±0.86° at 0 s and 11.63°±0.57° and 9.77°±1.32° at 1 s, respectively. The remarkable difference in the CA_{app} at 0 s between OA and TO can be attributed to the stronger affinity of the SG membrane to OA than TO. The CA_{app} at 0 s for both components decreased under SC-CO_2 compared to those under atmospheric conditions. This decrease was greater for OA, which can be due to the higher solubility and the lower interfacial tension of the OA in SC-CO_2 than TO. The exposure of the SG membrane to SC-CO_2 causes plasticization and swelling, which may increase its interactions with the lipids. The findings indicate that SC-CO_2 enhances the wetting behavior of the SG membrane with OA and thus SG membrane coupled with SC-CO_2 may have potential to separate OA from complex lipid mixtures.

INTRODUCTION

Reverse osmosis (RO) polymeric membranes can be used in combination with supercritical carbon dioxide (SC-CO_2) as a solvent. SC-CO_2 reduces the viscosity of the complex liquid mixture, allowing the membrane to fractionate mixtures, which would otherwise not be possible at ambient pressure. In addition, the membrane adds a fractionation step to separate mixtures, which would not be possible with SC-CO_2 alone when the solubilities of their components are similar. This approach has been used to fractionate lipids [1-3]. The separations observed were largely due to the affinity of the membrane to the components in the mixture and the permeability of the membrane under the conditions used. However, although the RO membranes used in SC-CO_2 fractionations have been characterized before and after exposure to SC-CO_2 [4], there is a lack of

information about the phenomena occurring on the membranes while being exposed to SC-CO_2 during processing. The interactions between the components in the mixture and the membrane under SC-CO_2 environment can be studied by the determination of the apparent contact angle (CA_{app}) of a drop on the membrane surface and by the spreading coefficient ($S_{L/S}$) of the liquid (L) on the solid (S) surface. When a liquid is in contact with a surface, it forms an angle θ with that surface, which is the result of the mechanical equilibrium among the three surface tensions, *e.g.*, the liquid surface tension (γ_{LA}), the solid surface tension (γ_{SA}), and the liquid–solid interfacial tension (γ_{SL}), as related through the Young's equation [5]:

$$\gamma_{LA} \times cos\theta = \gamma_{SA} - \gamma_{SL} \quad (1)$$

Contact angle measurements have been performed for different surfaces either for water in CO_2 atmosphere or for CO_2 in water atmosphere [6-8]. The contact angles of water in CO_2 atmosphere were measured both on a glass surface [6] and on polystyrene thin films [7]. In both cases, the contact angle increased significantly up until pressures close to the vapor pressure of CO_2, while pressurizing the system above the vapor pressure resulted only in a moderate increase in contact angle [6,7]. Saraji et al. [8] measured the contact angle of a CO_2 bubble on a quartz surface in water atmosphere, and reported that both advancing and receding contact angles increased from the CO_2 subcritical to the supercritical region, with a sharp increase near the critical point. However, there is a lack of information on the contact angle and spreading coefficient of lipids on membranes under SC-CO_2 atmosphere.

When the solid surface where the drop is deposited is not ideal (*e.g.*, has roughness), the angle formed is refered to as the apparent contact angle (CA_{app}) [9]. The CA_{app} can be easily determined by applying the B-spline snake method to captured video frames over the first moments of contact of the drop on the surface, while the same method is applied to the pendant drop at the tip of the needle before detaching to determine γ_{LA} [10]. This method applies parametric spline curves (piecewise-polynomial functions consisting of concatenated polynomial segments) to moving images to find the contour of the drop and calculate both CA_{app} and γ_{LA}. The drop of the liquid under study first contacts the surface but it may or may not adhere to it. The work necessary to separate the drop from the surface is referred to as the work of adhesion (W_A), which represents the affinity between the liquid and the surface [11]. It can be determined from Eq. 2:

$$W_A = \gamma_{LA} \times (\cos\theta + 1) \quad (2)$$

However, the behavior of the liquid on the surface is not determined only by the work of adhesion, but also by the work of cohesion (W_C). W_C represents the work required to produce two unit areas of interface from an original unbroken column of the liquid, *e.g.*, how likely a droplet is to remain intact [11]. It is expressed by:

$$W_C = 2 \times \gamma_{LA} \quad (3)$$

Finally, the spreading coefficient is obtained by subtracting the work of cohesion from the work of adhesion (Eq. 4). It represents the wettability of the surface by the liquid. If $S_{L/S}$ is larger than zero, the liquid spreads spontaneously on the surface to form a thin film [11].

$$S_{L/S} = W_A - W_c \quad (4)$$

The wetting behavior of lipids on RO membranes in SC-CO_2 environment is not known. Thus, the aim of this study was to determine the CA_{app} of oleic acid (OA) and triolein (TO) under atmospheric (22°C/0.1 bar) and SC-CO_2 (40°C/120 bar) environments on a commercial SG membrane over time (0-1 s). This parameter was correlated with the spreading coefficient through the work of adhesion and cohesion of the system to establish the wetting regime (partial or complete wettability) of OA and TO on SG membrane within the SC-CO_2 environment.

MATERIALS AND METHODS

Materials

SG membrane was provided by GE Osmonics Inc. (Minnetonka, MN, USA). OA (purity of 100%) and TO (purity ≥75%) were purchased from VWR International (Mississauga, ON, Canada). Both OA and TO were stored in amber bottles under nitrogen at 4˚C. Liquid CO_2 (purity of 99.9%, moisture content < 3 ppm) and nitrogen (purity of 99.998%) were obtained from Praxair Canada Inc. (Mississauga, ON, Canada). Water purified by Milli-Q® ultrapure water purification system (EMD Millipore, Billerica, MA, USA) was used to validate the system. Food grade anhydrous ethanol (EtOH) (Commercial Alcohol, Winnipeg, MB, Canada) was used for cleaning.

Apparatus to measure apparent contact angle

The experimental apparatus custom-built in our lab, which was previously reported for the determination of interfacial tension [12] was modified to measure contact angle. The system (Fig. 1) was equipped with a high pressure view cell (200 mL, ID=40 mm, Nova-Swiss, Effretikon, Switzerland), which was connected to a heating jacket and placed inside a temperature controlled air bath; both heating elements were separately monitored by means of J-type thermocouples connected to controllers (Chromalox, Pittsburgh, PA, USA). The pressure and temperature of the fluid inside the view cell were measured using a digital gauge (GE Druck, Leicester, UK) and a thermocouple (J-type) connected to controller, respectively.

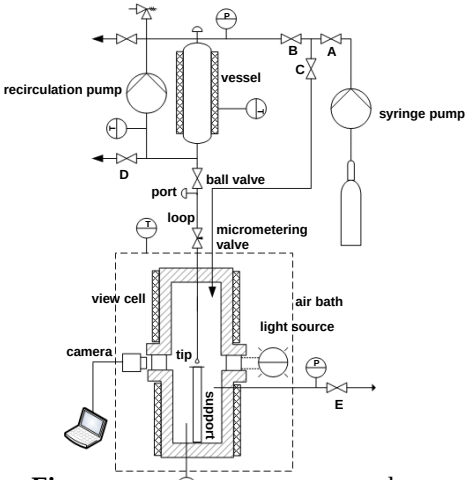

Fig the apparatus used for contact angle measurements. A, B, C, D, E are needle valves.

The sessile drops of OA and TO with and without SC-CO_2 were measured on a flat sheet of un-washed membrane (SG), placed on a stainless steel support inside the view cell. The position of the support was adjusted at the center of the view cell window (diameter of 5 mm) by means of a screw at the bottom. To verify that the membrane was mounted properly, the difference in θ between the right and left edges of the drop was measured (ImageJ software), and when this difference was less than 2° it was considered to be placed correctly. The drop was generated using two valves (one ball valve and one micrometering valve), which were installed on the tubing (loop) between the top reservoir vessel and the bottom view cell. The temperature of the tube was kept constant through a heating rope, which was connected to a controller and monitored by a thermocouple. A stainless steel capillary (OD=0.4572 mm, wall thickness=0.1 mm) (Type 304 SS dispensing needle 26 Gauge, McMaster-Carr, Atlanta, GA, USA) was connected to the end of the tubing using a fitting and a luer lok connector to create the drop. The capillary position was adjusted at the center of the view cell. Specifically, for the measurements under supercritical conditions, the OA or TO was saturated with SC-CO_2 (drop phase) in the top reservoir vessel (30 mL). To ensure the equilibration and homogenization of the saturated drop phase (solute and SC-CO_2) a recirculation pump (LEWA, EK-1-05MM, Leonberg, Germany) was used. The top reservoir, the tubes in the recirculation loop and the pump head were heated with heating ropes and separately monitored by means of thermocouples connected to temperature controllers. The pressure in the top reservoir was measured with a gauge (Swagelok, Solon, Ohio, USA). The system was pressurized with CO_2

using a syringe pump (Teledyne ISCO Inc., Model 260D, Lincoln, NE, USA).

The images of the drops were recorded by a CMOS camera (A602f, Basler Vision Technologies, Ahrensburg, Germany) equipped with a telecentric microscope lens with a zoom factor of up to 4.5 (VZM 450, Edmund Optics, Barrington, NJ). A fiberoptic light source (Intralux 4000, Volpi, Schlieren, Switzerland) and an opal diffuser (NT46-165, Edmund Optics, Barrington, NJ) were used to illuminate the drops. The videos were captured during 2 min using Virtual VCR free software (avi file format) and converted to frames using a free software (Free video). The frames were analyzed by ImageJ free software using the B-Spline plugin to determine the contact angle (minimum 10 knots were selected for each drop profile).

Before each contact angle measurement, the system was cleaned multiple times by recirculating first EtOH, then CO_2 + EtOH at 280 bar and 40˚C and in the end flushed with pure SC-CO_2 at 280 bar and 40˚C to remove residual solutes, EtOH, and air. The membrane support was washed and soaked with EtOH and then dried with compressed air. Contact angle measurements were performed in triplicate.

CA measurement at atmospheric conditions

First, OA or TO (20 mL) was injected into the loop using a disposable plastic syringe, through a port connected to the tube. After filling the loop, the capillary was flushed with OA or TO by fully opening the micrometering valve. Thereby, the tubing connecting to capillary and valve were rinsed and filled with the solute, while removing the air. The micrometering valve was closed after ~ 5 mL of solute passed through the capillary tip. Then, the light source was turned on and the membrane was placed properly on the support inside the view cell. Video recording was started prior to drop formation. To generate a drop suspended at the capillary tip and the sessile drop, the micrometering valve was opened slowly. All the measurements of contact angle in air were performed at 22°C/0.1 bar.

CA measurement at supercritical conditions

Prior to loading the solute (25 mL) in the top reservoir, the temperature controllers for the different parts of the whole system were set at 40˚C. Then, needle valves A and B (Fig. 1) were opened to pressurize the top part with pure SC-CO_2 at 120 bar, after which they were closed. The recirculation pump was turned on at 40 Hz for 2 h to reach equilibrium. Simultaneously, the light source was turned on, the membrane was placed on the support inside the view cell, and the micrometering valve was opened. The view cell was then pressurized with SC-CO_2 at 120 bar by opening the needle valves A and C (Fig. 1), until reaching the target pressure, after which they were closed. After reaching equilibrium (~ 2 h) in the top reservoir (saturated drop phase) and view cell (surrounding phase) the recirculation pump was turned off. Prior to drop formation, the micrometering valve was closed and the ball valve was opened to fill the loop with the CO_2-saturated lipid phase, then the camera was started to record the video. The micrometering valve was opened slowly to generate a drop suspended at the capillary tip followed by the sessile drop. The depressurization of the view cell was started by closing the ball valve and opening the micrometering and needle valve E (Fig. 1). Meanwhile, the top reservoir vessel was depressurized by opening the needle valve D (Fig. 1).

RESULTS

The methodology was validated by measuring the CA_{app} of milli-Q water on washed SG membrane (the membrane was washed according to Akin and Temelli [4]) at atmospheric conditions. The CA_{app} of water on washed SG membrane was 66°±0.98°, which was in agreement

with 69.3°±2° reported by Akin and Temelli [4]. The CA_{app} was also measured on un-washed SG membranes at atmospheric conditions; however, it was lower (57°±1.45°) compared to that on washed membrane. The increased hydrophilicity of the membrane surface may be due to the presence of contaminants. According to Tang et al. [13] and Akin and Temelli [4], traces of sulfonic groups were detected using FTIR at 1040 cm^{-1}, which were removed after the membrane was washed.

The maximum value of CA_{app} on SG membrane at atmospheric and supercritical conditions (40°C/120 bar) for OA (Fig. 2A) and TO (Fig. 2B) was obtained at 0 s when the drop touched the SG membrane. The CA_{app} values decreased sharply until 0.7 s for OA and 0.3 s for TO, followed by reaching a plateau.

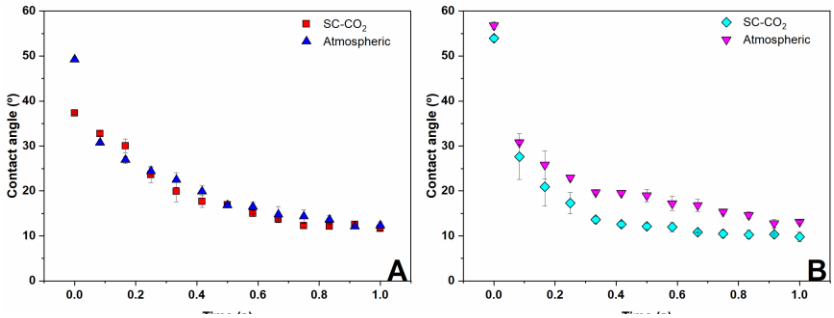

Figure 2. CA_{app} for (A) OA and (B) TO in atmospheric and SC-CO_2 environment as a function of time. Error bars represent the standard deviation based on triplicate measurements.

The CA_{app} for OA and TO at atmospheric conditions were 49.74°±0.64° and 56.80°±1.05° at 0 s and 12.26°±1.07° and 13.10°±0.46° at 1 s, respectively. The higher wettability of OA than TO at atmospheric conditions on SG membrane is due to the higher affinity of the selective layer of SG towards more oleophilic components. Akin and Temelli [4] have reported the presence of hydrophilic groups -OH and -NH on the surface of SG membrane. Furthermore, the CA_{app} results using milli-Q water suggested that the un-washed SG membrane surface is relatively hydrophilic, thereby, it could explain the higher CA_{app} obtained for TO compared to OA. Under SC-CO_2 environment, similar trends were observed where the CA_{app} for OA was also lower than that for TO. Specifically, the CA_{app} for OA and TO were 37.33°±0.27° and 53.92°±0.86° at 0 s and 11.63°±0.57° and 9.77°±1.32° at 1 s, respectively. Thereby, the higher wetabillity of OA compared to TO on un-washed SG membrane under SC-CO_2 environment confirmed the findings of Araus and Temelli [3], who reported that OA permeated preferentially through the un-washed SG membrane rather than TO at 120 bar and at 40°C.

As shown in Figure 2, the CA_{app} for both lipids decreased in presence of SC-CO_2 when compared to atmospheric conditions. At 0 s, the CA_{app} for OA and TO dropped 12.41° and 2.88°, respectively. These results suggest that the exposure of SG membrane to SC-CO_2 increased the wettability of both lipids on the SG membrane. This increase may be attributed to the ability of SC-CO_2 to penetrate the polymeric membrane and change its structure due to swelling and plasticization effects. Such phenomena can reduce the interactions between the polymer chains on the membrane or increase the interactions between CO_2 and the membrane [14], thereby, causing a reduction in the contact angle value. Also, the higher affinity and wettability or lower CA_{app} for OA than that for TO on the SG membrane under SC-CO_2 environment can be explained by the preferential interactions between the polar functional groups (-NH and -OH) on the polymeric membrane, the fatty acid, and quadrupolar CO_2. Moreover, the effect of SC-CO_2 on the CA_{app} of

lipids on un-washed membrane may be attributed to several effects linked to the mass transfer between the drop and surrounding phases, or diffusion of solutes from the CO_2-saturated drop phase to the surrounding phase, which might affect the interfacial tension, spreading coefficient, and contact angle. For example, Seifried and Temelli [12] reported the interfacial tension (γ_{LA}) of fish oil triglycerides and fatty acid ethyl esters in the presence of CO_2 at 40, 50 and 70°C and pressures of up to 250 bar, where the interfacial tension of both components decreased as pressure increased due to a higher amount of CO_2 adsorbed onto the interface at higher densities.

Figure 3 shows the $S_{L/S}$ for OA and TO under atmospheric conditions and in the presence of SC-CO_2 based on the difference between W_A (Fig. 4) and W_C (Eq. 4). To determine the W_A and W_C, information reported in the literature was used for interfacial tension and densities of drop and surrounding phases [15-20]. The W_C calculated in the presence of CO_2 was lower than that in air. For example, the W_C for OA and TO at higher pressure in SC-CO_2 were 7.13 mN/m and 16.36 mN/m while at atmospheric pressure they were 63.6 mN/m and 64.82 mN/m, respectively.

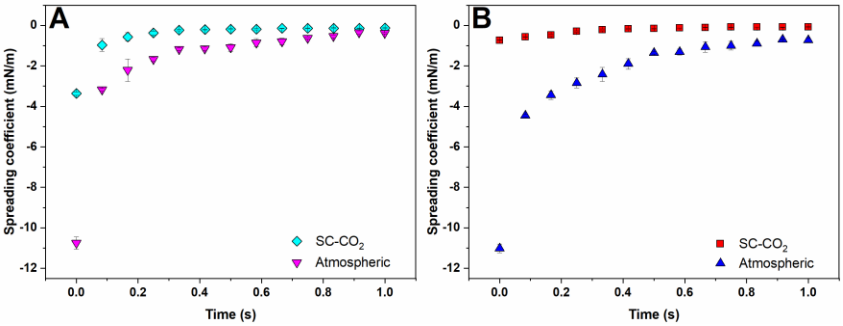

Figure 3. Spreading coefficient for (A) OA and (B) TO in atmospheric and SC-CO_2 environment as a function of time. Error bars represent the standard deviation based on triplicate measurements

Under atmospheric conditions the $S_{L/S}$ for OA and TO is more negative than in the presence of SC-CO_2, indicating a partial wetting for both compounds on un-washed SG membrane (Fig. 3). However, the $S_{L/S}$ for OA and TO in SC-CO_2 environment were enhanced (less negative), indicating higher wettability and a decrease in CA_{app} on the membrane surface (Fig. 3), thereby the liquid can spread more spontaneously over the surface of SG membrane. For example, the $S_{L/S}$ for OA at 120 bar and 40°C ranged from -0.71 mN/m (at 0 s) to -0.071 mN/m (at 1 s) while at atmospheric conditions it ranged from -11.01 mN/m (at 0 s) to -0.62 mN/m (at 1 s). Thus, the $S_{L/S}$ is affected by the presence of SC-CO_2, which decreased the interfacial tension (γ_{LA}) with increased pressure, and it might also modify the value of γ_{SA} due to the dissolution of drop phase in the SC-CO_2 phase [6]. The high pressure surrounding phase in contact with the membrane surface could change its surface free energy compared to that under atmospheric conditions, modifying the preferential interactions between the drop phase with the solid phase (membrane) and the value of CA_{app}.

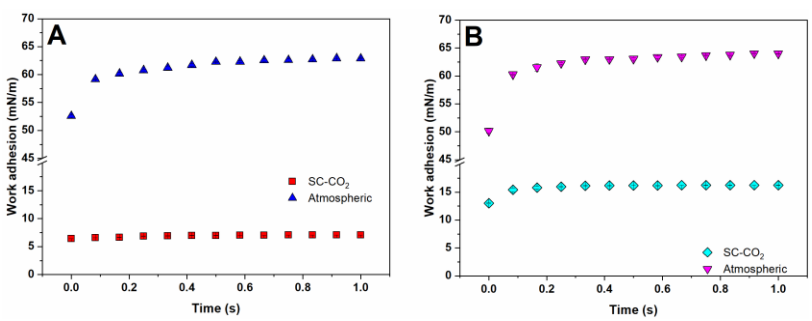

Figure 4. W_A for (A) OA and (B) TO in atmospheric and SC-CO_2 environment as a function of time. Error bars represent the standard deviation based on triplicate measurements.

CONCLUSION

The CA_{app} for OA and TO at atmospheric (22°C/0.1 bar) and supercritical (SC-CO_2 at 40°C/120 bar) conditions was measured by using the B-spline snake method for a sessile drop on un-washed SG membrane. The system and methodology were validated by measuring the CA_{app} for milli-Q water on washed SG membrane at atmospheric conditions. The CA_{app} of milli-Q water on un-washed SG membrane was lower that on washed SG membrane. This was attributed to the presence of contaminants, which decreased the hydrophobicity of the membrane surface. The CA_{app} for OA and TO in SC-CO_2 environment was lower than those at atmospheric conditions. Besides, the spreading coefficient under SC-CO_2 was less negative compared to that at atmospheric conditions. Therefore, the lower CA_{app} and higher wettability for TO and OA on un-washed SG membrane were obtained in pure SC-CO_2 environment. These results can be attributed to the mass transfer occurring between the lipid drop and the surrounding SC-CO_2 phase, which might modify the contact angle. Moreover, the unsaturated SC-CO_2 surrounding phase might change the surface free energy of membrane surface, thereby increasing its interaction with the drop phase. Also, the effect of swelling on SG membrane by exposure to SC-CO_2 may increase the interactions between the polymer chains on the membrane or increase the interactions between CO_2 and the membrane, thus, modifying the contact angle value. The findings address the lack of information regarding the contact angle in SC-CO_2 environment, which can be applied in the optimization of separation processes involving SG membranes.

ACKNOWLEDGEMENTS

The authors acknowledge the Natural Sciences and Engineering Research Council of Canada (NSERC)-Discovery Grants Program (RGPIN-2017-04384) for financial support and GE Osmonics Inc. for providing the membranes.

REFERENCES

[1] ARTZ W., KINYANJUI T., CHERYAN M., Deacidification of soybean oil using supercritical fluid and membrane technology, J. Am. Oil Chem. Soc., 82, 2005, 803–808.
[2] DE MOURA J., GONÇALVES L., SARMENTO L., PETRUS J., Purification of structured lipids using SC-CO_2 and membrane process, J. Memb. Sci., 299, 2007, 138–145.
[3] ARAUS K., TEMELLI F., Separation of major and minor lipid components using supercritical CO_2 coupled with cross- flow reverse osmosis membrane filtration, J. Memb. Sci., 551, 2018, 333–340.
[4] AKIN O., TEMELLI F., Probing the hydrophobicity of commercial reverse osmosis membranes produced by interfacial polymerization using contact angle, XPS, FTIR, FE-SEM and AFM, Desalination, 278, 2011, 387–396.
[5] LAW K-Y., ZHAO H., What do contact angles measure?, in: Surface wetting: characterization, contact angle, and fundamentals, Springer, Cham, Switzerland, 2016: pp. 99–121.
[6] DICKSON J., GUPTA G., HOROZOV T., BINKS B., JOHNSTON K., Wetting phenomena at the CO_2/water/glass interface, Langmuir, 22, 2006, 2161–2170.

[7] LI Y., PHAM J., JOHNSTON K., GREEN P., ARBOR A., Contact angle of water on polystyrene thin films: Effects of CO_2 environment and film thickness, Langmuir, 23, 2007, 9785–9793.
[8] SARAJI S., GOUAL L., PIRI M., PLANCHER H., Wettability of supercritical carbon dioxide/water/quartz systems: Simultaneous measurement of contact angle and interfacial tension at reservoir conditions, Langmuir, 29, 2013, 6856–6866.
[9] LAW K-Y., ZHAO H., Wetting on rough surfaces, in: Surface wetting: characterization, contact angle, and fundamentals, Springer, Cham, Switzerland, 2016: pp. 55–98.
[10] STALDER A., KULIK G., SAGE D., BARBIERI L., HOFFMANN P., A snake-based approach to accurate determination of both contact points and contact angles, Colloids Surfaces A Physicochem. Eng. Asp., 286, 2006, 92–103.
[11] ROSEN M., KUNJAPPU J., Wetting and its modification by surfactants, in: Surfactants interfacial phenomena, John Wiley and Sons, Hoboken, 2012: pp. 272–307.
[12] SEIFRIED B., TEMELLI F., Interfacial tension of marine lipids in contact with high pressure carbon dioxide, J. Supercrit. Fluids, 52, 2010, 203–214.
[13] TANG C., KWON Y-N., LECKIE J., Effect of membrane chemistry and coating layer on physiochemical properties of thin film composite polyamide RO and NF membranes, Desalination, 242, 2009, 149–167.
[14] ISMAIL A., LORNA W., Penetrant-induced plasticization phenomenon in glassy polymers for gas separation membrane, Sep. Purif. Technol., 27, 2002, 173–194.
[15] LOCKEMAN C., Interfacial tensions of binary systems carbon dioxide-oleic acid, carbon dioxide-methyl myristate, and carbon dioxide-methyl palmitate and of the ternary system carbon dioxide-methyl myristate-methyl palmitate at high pressures, Chem. Eng. Process. Process Intensif., 33, 1994, 193–198.
[16] LOCKEMAN C., High-pressure phase equilibria and densities of the binary mixtures carbon dioxide-oleic acid, carbon dioxide-methyl myristate, and carbon dioxide-methyl palmitate and of the ternary system carbon dioxide-methyl myristate-methyl palmitate at high pressures, Chem. Eng. Process. Process Intensif., 33, 1994, 171–187.
[17] MELO-ESPINOSA E., SÁNCHEZ-BORROTO Y., ERRASTI M., PILOTO-RODRÍGUEZ R., SIERENS R., ROGER-RIBA J., CHRISTOPHER-HANSEN A., Surface tension prediction of vegetable oils using artificial neural networks and multiple linear regression, Energy procedia, 57, 2014, 886–895.
[18] AYDAR A., RODRIGUEZ-MARTINEZ V., FARKAS B., Determination and modeling of contact angle of canola oil and olive oil on a PTFE surface at elevated temperatures using air or steam as surrounding media, LWT -Food Sci. Technol., 65, 2016, 304–310.
[19] LEMMON E., MCLINDEN M., FRIEND D., Thermophysical properties of fluid systems, in: P.J. Linstrom, W.G. Mallard (Eds.), NIST Chemistry WebBook, NIST Standard Reference Database Number 69, National Institute of Standards and Technology, Gaithersburg MD, 20899. ⟨http://webbook.nist.gov.login.ezproxy.library.ualberta.ca⟩ (Accessed on July 7, 2017).
[20] ILIEVA P., KILZER A., WEIDNER E., Measurement of solubility, viscosity, density and interfacial tension of the systems tristearin and CO_2 and rapeseed oil and CO_2, J. Supercrit. Fluids, 117, 2016, 40–49.